THE JOURNAL OF BIOLOGICAL CHEMISTRY VOL. 284, NO. 13, pp. 8292–8300, March 27, 2009

N-Glycan Moieties in Neonatal Fc Receptor Determine Steady-state Membrane Distribution and Directional Transport of IgG*[S]

Received for publication, July 31, 2008, and in revised form, January 7, 2009 Published, JBC Papers in Press, January 21, 2009, DOI 10.1074/jbc.M805877200

Timothy T. Kuo[‡], Eric J. de Muinck[‡], Steven M. Claypool[‡], Masaru Yoshida[‡], Takashi Nagaishi[‡], Victoria G. Aveson[‡], Wayne I. Lencer[§], and Richard S. Blumberg[‡1]

From the [‡]Department of Gastroenterology, Brigham & Women's Hospital and Harvard Medical School, and the [§]Department of Gastroenterology, Children's Hospital and Harvard Medical School, Boston, Massachusetts 02115

The neonatal Fc receptor (FcRn) is a major histocompatibility complex class I-related molecule known to protect IgG and albumin from catabolism and transport IgG across polarized epithelial cells in a bidirectional manner. Previous studies have shown species-specific differences in ligand binding, IgG transport direction, and steady-state membrane distribution when expressed in polarized epithelial cells. We hypothesized that these differences may be due to the additional *N*-glycans expressed on the rat FcRn, because *N*-glycans have been proposed to function as apical targeting signals, and that two of the *N*-glycan moieties have been shown to contribute to the IgG binding of rat FcRn. A panel of mutant human FcRn variants was generated to resemble the *N*-glycan expression of rat FcRn in various combinations and subsequently transfected into Madin-Darby canine kidney II cells together with human β2-microglobulin. Mutant human FcRn clones that contained additional *N*-glycan side-chain modifications, including that which was fully rodentized, still exhibited specificity for human IgG and failed to bind to mouse IgG. At steady state, the mutant human FcRn with additional *N*-glycans redistributed to the apical cell surface similar to that of rat FcRn. Furthermore, the rodentized human FcRn exhibited a reversal of IgG transport with predominant transcytosis from an apical-to-basolateral direction, which resembled that of the rat FcRn isoform. These studies show that the *N*-glycans in FcRn contribute significantly to the steady-state membrane distribution and direction of IgG transport in polarized epithelia.

The neonatal Fc receptor (FcRn)[2] was originally proposed by Brambell and colleagues to be the Fc receptor responsible for transfer of IgG through neonatal rodent intestinal epithelium and yolk sac of pregnant rabbits more than three decades ago (1). These functional properties were confirmed to be mediated by FcRn with the subsequent isolation from neonatal rat intestinal brush borders followed by the cloning of the rat homologue identified as a 50-kDa major histocompatibility complex class I-related heavy chain in non-covalent association with a 12-kDa subunit consistent with β2-microglogbulin (β2m) (2). Since that time, the structural and functional properties of FcRn have been identified for the human, rat, mouse, bushtail possum, pig, monkey, sheep, cow, and horse isoforms with the majority of information available from human and rodent sources (3). In all species identified, a hallmark feature of FcRn is pH-dependent IgG binding. FcRn binds its ligand IgG at acidic pH, but not at neutral pH, due to the conserved presence of basic histidine residues within the CH2-CH3 domain interface of the Fc domain of IgG, which interact with corollary acidic residues within the α2 and α3 domains of FcRn (4). FcRn is developmentally regulated especially in rodents where it is expressed at high levels within the intestinal epithelium during the first 2 weeks of life prior to weaning where it functions in the passive acquisition of IgG from breast milk (5, 6). Despite its designation as neonatal, FcRn is expressed in many tissues and cell types beyond neonatal life in most animal species where it has been identified. FcRn has been detected in numerous types of polarized epithelia, including those from the intestines, lung, breast, and kidney, as well as other parenchymal cells, including hepatocytes, endothelial cells, and hematopoietic cells, where it is expressed in dendritic cells, monocytes, macrophages, polymorphonuclear leukocytes, and, perhaps, B cells (7, 8). FcRn protects monomeric IgG and albumin from degradation in both parenchymal and hematopoietic cells, is responsible for the bidirectional transcytosis of IgG and IgG antigen/antibody complexes across polarized epithelia, and, finally, directs immune complexes to lysosomes in dendritic cells for facilitation of antigen presentation (9, 10).

Despite overall similarities in structure with the presence of extracellular α1–3 domains, a transmembrane anchor and a short cytoplasmic tail of ~42 amino acids, detailed amino acid comparisons reveal significant differences, which may account for reported functional variation between FcRn homologues

* This work was supported, in whole or in part, by National Institutes of Health Grants DK071798 (to T. T. K.) and DK053056 (to R. S. B. and W. I. L.). This work was also supported by the American Liver Foundation, the Crohn's & Colitis Foundation of America (to M. Y. and T. N.), and Harvard Digestive Diseases Center Grant P30 DK034854 (to R. S. B. and W. I. L.). The costs of publication of this article were defrayed in part by the payment of page charges. This article must therefore be hereby marked "*advertisement*" in accordance with 18 U.S.C. Section 1734 solely to indicate this fact.

[S] The on-line version of this article (available at http://www.jbc.org) contains supplemental Figs. S1–S4.

[1] To whom correspondence should be addressed: Brigham and Women's Hospital, Gastroenterology Division, Dept. of Medicine, 75 Francis St. Boston, MA 02115. Tel.: 617-732-6917; Fax: 617-264-5185; E-mail: rblumberg@partners.org.

[2] The abbreviations used are: FcRn, neonatal Fc receptor; β2m, β2-microglobulin; h, human; r, rat; MDCK, Madin-Darby canine kidney cell; HA, hemagglutinin; CHAPS, 3-[(3-cholamidopropyl)dimethylammonio]-1-propanesulfonic acid; HBSS, Hanks' balanced salt solution; PNGase F, *N*-glycosidase F; Endo H, endoglycosidase H; WT, wild type.

among different species. For example, rat and mouse FcRn are known to be "promiscuous" in their ability to bind various species of IgG, including human and rabbit. In contrast, human FcRn is more limited in its cross-species IgG binding (11). "Murinization" of human FcRn by Ward and colleagues has demonstrated that sequences at residue 137 and between 121–132 within the α2 domain regulate the ability of human FcRn to exhibit a broad range of cross-species binding to IgG and thus account for this property of mouse FcRn (12). Thus, differences in FcRn structure between the various homologues of FcRn can be utilized to focus on regions of the molecule that may control the functions of FcRn and its mechanisms.

One of the major structural differences observed between human and rodent FcRn is the presence of a single *N*-glycan motif in human FcRn within the α2 domain compared with rodent (mouse and rat) FcRn, which contains three additional *N*-glycan carbohydrate modifications within the α1, α2, and α3 domains (supplemental Fig. S1). This is interesting because the rat *N*-glycans have been implicated in FcRn-IgG interactions (7). Specifically, the *N*-glycan located at Asn-128 within the α2 domains of rat FcRn has been observed to contact Fc. Human FcRn does not contain this homologous carbohydrate residue (13). Furthermore, the crystal structure of FcRn has shown that the interaction between the *N*-glycan associated with Asn-128 forms a "carbohydrate handshake" that helps stabilize the association of FcRn with IgG (14). Still, the physiologic significance of the *N*-glycans that are associated with FcRn remains unclear. It is interesting that *N*-glycans have been suggested to be apical targeting signals in other proteins (15). However, nothing is known with respect to FcRn.

Most studies of both human and rat FcRn trafficking in epithelial cells have focused on the cytoplasmic tail, which has revealed the critical role of this domain in basolateral membrane targeting, endocytosis, and transcytosis. Deletion of the hFcRn cytoplasmic tail or point mutations of membrane proximal sites that are functional in calmodulin binding diminish preferential basolateral targeting and redistribute hFcRn to the apical membrane together with a decrease in IgG transcytosis (16, 17).

Similarly, studies of rat (r)FcRn in rat inner medullary collecting duct cells, a rat kidney epithelial cell line, have shown that deletion of the rFcRn cytoplasmic tail or mutation of serine-313, a site for phosphorylation, significantly diminishes apical-to-basolateral IgG transport (18). Mutations of the tryptophan and dileucine motif present within the rFcRn cytoplasmic tail results in increased apical expression due to decreased apical endocytosis (19). When rFcRn with green fluorescent protein at the cytoplasmic tail was expressed in Madin-Darby canine kidney (MDCK) II cells, endocytosis of rFcRn-green fluorescent protein was observed, but transport of wild-type Fc fragments did not occur (20). It is unclear whether this was due to structural interference of the green fluorescent protein domain with possible basolateral trafficking information within the FcRn cytoplasmic tail. Another study has also emphasized the significance of the cytoplasmic tail in membrane targeting. When the rFcRn cytoplasmic tail is attached to the ectodomain of FcγRII, the cytoplasmic tail is able to direct the bidirectional transcytosis of IgG across MDCK cells (21). To date, no prior studies have evaluated apical targeting signals or non-cytoplasmic tail motifs that may be responsible for either human or rodent FcRn trafficking in polarized epithelia.

TABLE 1

Primers used in site-directed mutagenesis utilizing overlapping primers

The primers used contain nucleotides sequences described in Fig. 1 to add various numbers and combinations *N*-glycan(s) described in supplemental Fig. S2.

1-hFcRn	5′ – GGTCCCATTTATTTGGTCTCCAAGGCTTTGAAAGCTTCC – 3′ 5′ – GAGACCAAATAAATGGGACCTACACTCTGCAGGGCCTGCT – 3′
1m-hFcRn	5′ – GGTCCCCTGTATTTGGTTCTCCAAGGCTTTGAAAGCTTCC – 3′ 5′ – GAGAACCAAATACAGGGGACCTACACGCTGCAGGGCCTGCT – 3′
3-hFcRn	5′ –ACTCCAGTTGCCTGTTCTTGGGTCGAAATTCATAAACTCCTC– 3′ 5′ – CCAAGAACAGGCAACTGGAGTGGGGACTGGCCCGAG – 3′
3m-hFcRn	5′ – ACTCCATTGTCCTGTTCTTGGGTCGAAATTCATAAACTCCTC – 3′ 5′ – CCAAGAACAGGACAATGGAGTGGAGACTGGCCCGAGGC – 3′
4- hFcRn	5′ – TGTGCTACAATTCCCTGAGCCAGCGGCCAGCCCATTC – 3′ 5′ – GGCTCAGGGAATTGTAGCACAGGCCCCAACAGTGACG – 3′
4m-hFcRn	5′ – TGTGCTACATTGTCCTGAGCCAGCGGCCAGCCCATTC – 3′ 5′ – GGCTCAGGACAATGTAGCACAGGCCCCAACAGTGACG – 3′
0-hFcRn	5′ – CACCGAGGTTTGGTCAGGGCCCAGTTCACA – 3′ 5′ – GGCCCTGACCAAACCTCGGTGCCCACCGCC – 3′

As described above, a major structural difference between rodent and human FcRn is the presence of four, rather than one, *N*-glycan carbohydrate side-chain modifications within the ectodomains of rodent FcRn. However, the functional role for these post-translational modifications is unknown. We therefore investigated the role of these residues by conferring them upon hFcRn, or "rodentization" of hFcRn, through the addition of amino acid residues into hFcRn that are associated with *N*-linked carbohydrate substitutions as would be observed in the rodent isoform. Our study shows that addition of the rodent *N*-glycans to the human homologue, irrespective of their number or location within hFcRn, did not allow for binding of hFcRn to rat IgG. However, rodentization of hFcRn resulted in apical redistribution of membrane-bound FcRn and reversal of the dominant vector of IgG transport associated with hFcRn (predominantly basal-to-apical membrane) to a direction that is typically associated with the rFcRn homologue (apical-to-basolateral membrane) (16, 18, 19).

EXPERIMENTAL PROCEDURES

Plasmid Construction—MDCK II-expressing human (h) FcRn and hβ2m were constructed as previously described (22). hFcRn with various mutations in *N*-glycans were created using site-directed mutagenesis by overlapping extension using PCR (23). The primers used for each mutation and amino acid sequence mutations of hFcRn that were created are summarized in Table 1 and Fig. 1. rFcRn and rat (r) β2m cDNA (both a kind gift from Dr. Pamela Bjorkman, California Institute of Technology, Pasadena, CA) were subcloned into pcDNA3.1 and pEF5/V6-HisA (Invitrogen), respectively. Similar to the previous human FcRn construct, an N-terminal hemagglutinin (HA) tag (5′-YPYDVPDYA-3′) following a major histocompat-

ibility complex class I signal peptide was inserted to precede the mature polypeptide of rat (r) FcRn (16, 22). The mutant hFcRn constructs were transfected into MDCK II cells stably expressing hβ2m as previously described. rFcRn and rβ2m were transfected into MDCK II cells as described previously (22). Stable clones were subsequently selected by ring cloning.

Antibodies—Monoclonal antibodies 12CA5 (mouse IgG2b) specific for HA, BBM.1 (mouse IgG) specific for both human and rat β2m, 1G3 (mouse IgG1) specific for rat FcRn, anti-GP135 (mouse IgG) specific for an apical marker in MDCK II cells, and anti-β-actin (Sigma, mouse IgG) were used as described previously (16). Polyclonal human and rabbit IgG antibodies (Lampire Biological Laboratories) were used for transcytosis studies. These polyclonal antibodies were first dialyzed in phosphate-buffered saline and subsequently filtered through a 0.22-μm membrane before use.

Cells—MDCK II cells with empty plasmid vectors, hFcRn mutant clones, and rFcRn were maintained in medium containing Dulbecco's modified Eagle's medium with 10% fetal bovine serum, and the appropriate mammalian selection antibiotics at 37 °C with 5% CO_2 environment. MH1C1, a rat liver cell line, was maintained in medium containing Ham's F-12 medium (Cellgro) with 15% horse serum and 2.5% fetal bovine serum at 37 °C with 5% CO_2 environment.

IgG Binding—Cells were lysed in CHAPS at pH 6.0 or 8.0 as described previously (22). Equal protein concentrations from the lysates were incubated with either 200 μg of human or mouse IgG (Lampire Biological Laboratories) for 2 h followed by incubation with protein G-Sepharose overnight at 4 °C. Following immunoprecipitation, the proteins were resolved on 12% SDS-PAGE gels under nonreducing conditions and subsequently transferred onto nitrocellulose membranes (Whatman) prior to detection by immunoblotting.

Cell Surface Biotinylation—Polarized cells were grown on 12-mm, 0.4-μm polycarbonate membrane Transwells (Corning, Inc.) for at least 72–96 h. Transepithelial resistance was measured before commencement of experiments with a resistance meter (World Precision Instrument, Inc.). The Transwells were washed with phosphate-buffered saline and subsequently incubated with 1 mg/ml biotin (Pierce) at either or both membrane surfaces for 30 min before washing and quenching as described previously (22). The membranes were then removed from the Transwells, and the cells lysed with radioimmune precipitation assay containing Complete protease inhibitors (Roche Applied Science) at pH 7.4 for 1 h. After centrifugation, postnuclear supernatants were harvested. Equal quantities of protein were used for the study, with 95% of the material used for incubation with avidin agarose for 24 h, and the remaining 5% used for lysate. Following immunoprecipitation, the proteins were resolved on 12% SDS-PAGE under reducing conditions. Densitometry analysis was performed using ImageJ software (National Institutes of Health).

IgG Transcytosis—Cells were grown to confluence on 12-mm, 0.4-μm polycarbonate membrane Transwells (Corning), and the transepithelial resistance was determined by resistance meter as described above. The Transwells were washed in Hanks' balanced salt solution (HBSS, Sigma), pH 6 and subsequently in pH 7.4. This was followed by a 20-min equilibration with HBSS, pH 6, at the side anticipated to receive hIgG and HBSS, pH 7.4, at the contralateral side of the monolayer. Human IgG (Lampire) equilibrated in HBSS, pH 6, was added to the input chamber of the Transwell and allowed to incubate for 120 min at 37 °C with 5% CO_2 environment. The output chamber fluid was then removed, and the hIgG concentrations were measured by enzyme-linked immunosorbent assay. For experiments using rabbit IgG blocking, rabbit polyclonal IgG (Lampire) equilibrated in HBSS, pH 6, was added at the time of HBSS, pH 6, equilibration prior to the addition of hIgG.

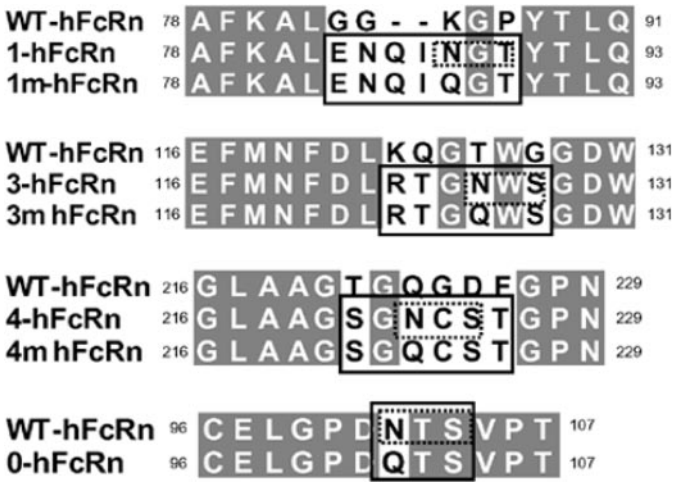

FIGURE 1. **Amino acid sequence of hFcRn clones.** Amino acid sequence of wild-type (WT) hFcRn and sequence mutations of hFcRn (*solid rectangular box*), which correspond to that of rFcRn sequence. The predicted glycosylation sequence for rFcRn is highlighted in *dashed rectangular box*. Corresponding non-glycosylation sequence, wherein conservative substitution of asparagine with glutamine, were created on "mutant" (*m*) clones: 1m-hFcRn, 3m-hFcRn, 4m-hFcRn, and 0-hFcRn clones.

Statistics—Statistical analysis was performed using Student's *t* test. $p < 0.05$ was determined to be significant.

RESULTS

Functional Expression of Human FcRn Mutants and Rat FcRn in MDCK II Cells—To generate mutant hFcRn expressing additional *N*-glycans that mimic those that are contained within rFcRn, nucleotide sequences of the corresponding hFcRn region were mutated to encode N*X*(T/S) to allow post-translational modification with *N*-glycan carbohydrate (supplemental Fig. S1 and Fig. 1). For each clone, a negative control was created by modifying the sequence to contain the motif Q*X*(T/S), which we defined as (m) mutant (Fig. 1). In this case, an asparagine residue was substituted with a conservative glutamine that does not allow for *N*-glycan addition. Different numbers, locations, and combinations of *N*-glycans were created as described schematically in supplemental Fig. S2. Using a similar mutagenesis method, hFcRn without any *N*-glycans was also generated as an additional control (0-hFcRn).

These human FcRn mutants and rat FcRn constructs were transfected into MDCK II cells that expressed the corresponding species of human or rat β2m, because we have previously found that this is substrate-limiting in MDCK II cells (22). The transfectants were then examined for expression of the corresponding proteins. As shown in Fig. 2*A* (*lane 4*), the wild-type

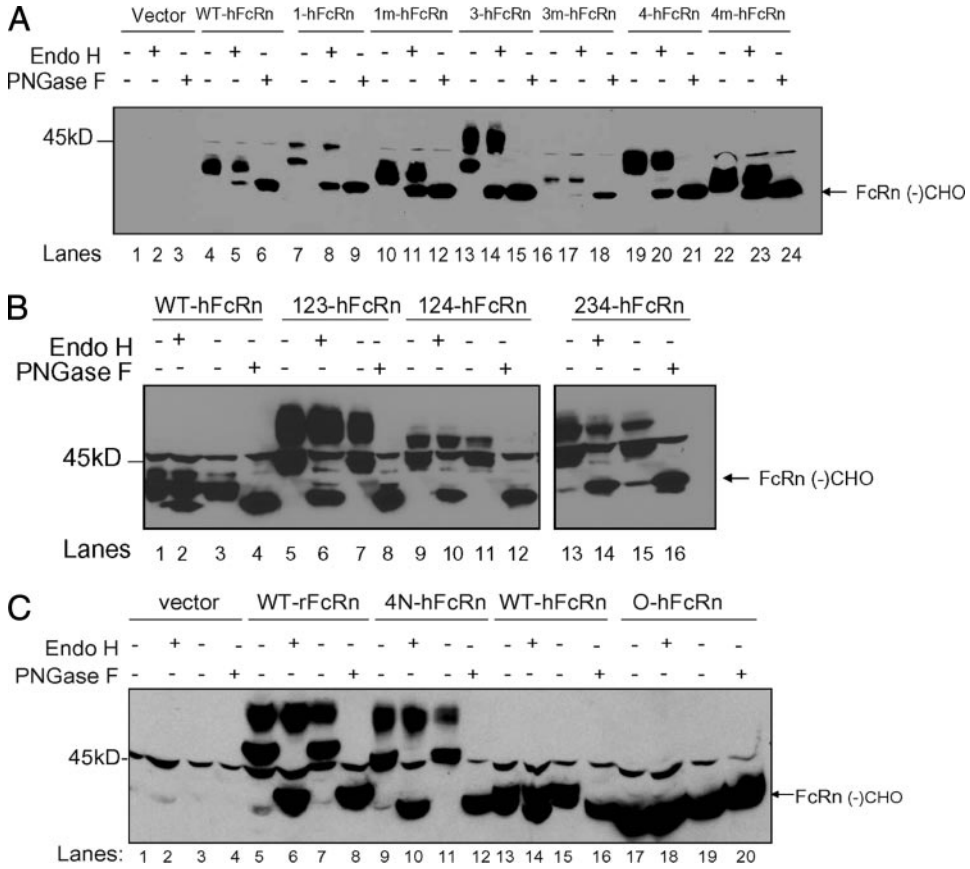

FIGURE 2. **Functional expression of WT-hFcRn and "rodentized" hFcRn clones.** Stable clones of hFcRn and mutant hFcRn clones were generated by transfection of MDCK II cells with hβ2m, and the lysates examined for expression of all transfected clones. Lysate incubation with Endo H removed high mannose *N*-glycan residues but not complex *N*-glycan residues, resulting in an upper band (hFcRn with complex *N*-glycans) and a lower band (hFcRn without any *N*-glycan residues, deglycosylated FcRn, "*FcRn(-)CHO*"). PNGase F removed all *N*-glycan residues, thus resulting in only a single lower band, representing deglycosylated FcRn, "*FcRn(-)CHO.*" The clones consisted of wild type hFcRn (*A*, lanes 4–6), hFcRn with one additional N-glycan (*A*, lanes 7–24), hFcRn with two addition N-glycans (*B*, lanes 5–16), "Rodentized" hFcRn with three additional N-glycans (*C*, lanes 9–12), wild-type rat FcRn (*C*, lanes 13–16), and hFcRn without any N-glycans (*C*, lanes 17–20).

human FcRn protein was observed as a band of ~40–43 kDa, which is consistent with the predicted molecular mass of hFcRn. As predicted, the addition of each *N*-glycan moiety increased the molecular mass of hFcRn by 1.5–3 kDa (Fig. 2*A*). As such, hFcRn that had been modified to contain an additional carbohydrate side-chain modification at the corresponding position within the α1 domain (1-hFcRn), α2 domain (3-hFcRn), or α3 domain (4-hFcRn) migrated as a band of ~45 kDa (Fig. 2*A*). hFcRn that had been mutated to contain the non-glycosylating sequence, QS(T/S), within the α1 (1m-hFcRn), α2 (3m-FcRn), and α3 (4m-hFcRn) domains expressed the same molecular masses as that of wild-type hFcRn (Fig. 2*A*, *lanes 10*, *16*, and *22*). All hFcRn clones and mutants expressed hβ2m (data not shown).

hFcRn, which encoded different combinations of rodent-like carbohydrate side-chain modifications, were also generated (supplemental Fig. S2). Characterization of these hFcRn isoforms after transfection into MDCK II cells are shown in Fig. 2*B*. These clones included hFcRn with two additional carbohydrate side-chain modifications at positions 1 and 3 (as per nomenclature described in supplemental Figs. S1 and S2) (123-hFcRn), positions 1 and 4 (124-hFcRn), and positions 3 and 4 (234-hFcRn). In comparison to WT-hFcRn (Fig. 2*B*, *lane 1*), with the addition of two *N*-glycan carbohydrates, all of these isoforms migrated as a glycoprotein of ~50 kDa (Fig. 2*B*, *lanes 5*, *9*, and *13*).

Finally, a fully rodentized version of hFcRn (4N-hFcRn) was created that contained *N*-glycan carbohydrate at positions 1, 2, 3, and 4 (supplemental Fig. S2). When expressed in MDCK II cells, the 4N-hFcRn migrated as a protein of ~52 kDa, which is identical to that of wild-type rat FcRn (Fig. 2*C*, *lane 5* and *9*). On the other hand, the hFcRn clone that had no *N*-glycans (0-hFcRn) migrated as a ~37-kDa protein (Fig. 2*C*, *lane 17*), which is the same molecular mass as all clones that had been subjected to peptide:*N*-glycosidase F (PNGase F) digestion, an enzyme that removes all *N*-glycan carbohydrate side chains, resulting in only the "deglycosylated" protein.

The characteristics of the *N*-glycan(s) expressed by the various FcRn isoforms created were characterized by sensitivity to endoglycosidase H (Endo H), which cleaves only high mannose carbohydrate residues from *N*-linked glycoproteins, and PNGase F, which cleaves all forms of *N*-glycan carbohydrate side-chain residues, including high mannose and complex *N*-glycan isoforms. The addition of Endo H resulted in deglycosylation of only high mannose FcRn isoforms but not that of FcRn with complex *N*-glycans and thus resulted in the generation of a band at ~37 kDa, which is consistent with a deglycosylated FcRn heavy chain (*arrow* in Fig. 2*A*, *lanes 5*, *8*, *11*, *14*, *17*, *20*, and *23*; Fig. 2*B*, *lanes 2*, *6*, *10*, and *14*; and Fig. 2*C*, *lanes 6*, *10*, and *13*). After Endo H digestion, in addition to the deglycosylated FcRn heavy chain, an upper band representing FcRn with complex *N*-glycans that remained resistant to Endo H digestion was detected in each clone examined. On the other hand, PNGase F removes both high mannose (immature) and complex (mature) *N*-glycans, resulting in only the deglycosylated FcRn heavy chain. In each case, PGNase F digestion resulted in complete digestion of all FcRn heavy chains leading to the generation of a deglycosylated hFcRn, which was of the same molecular weight as that of the 0-hFcRn heavy chain (Fig. 2*A*, *lanes 6*, *9*, *12*, *15*, *18*, *21*, and *24*; Fig. 2*B*, *lanes 4*, *8*, *12*, and *16*; and Fig. 2*C*, *lanes 8*, *12*, *16*, and *20*). All mutant hFcRn clones thus expressed *N*-glycans with both high mannose and complex *N*-glycan carbohydrate isoforms.

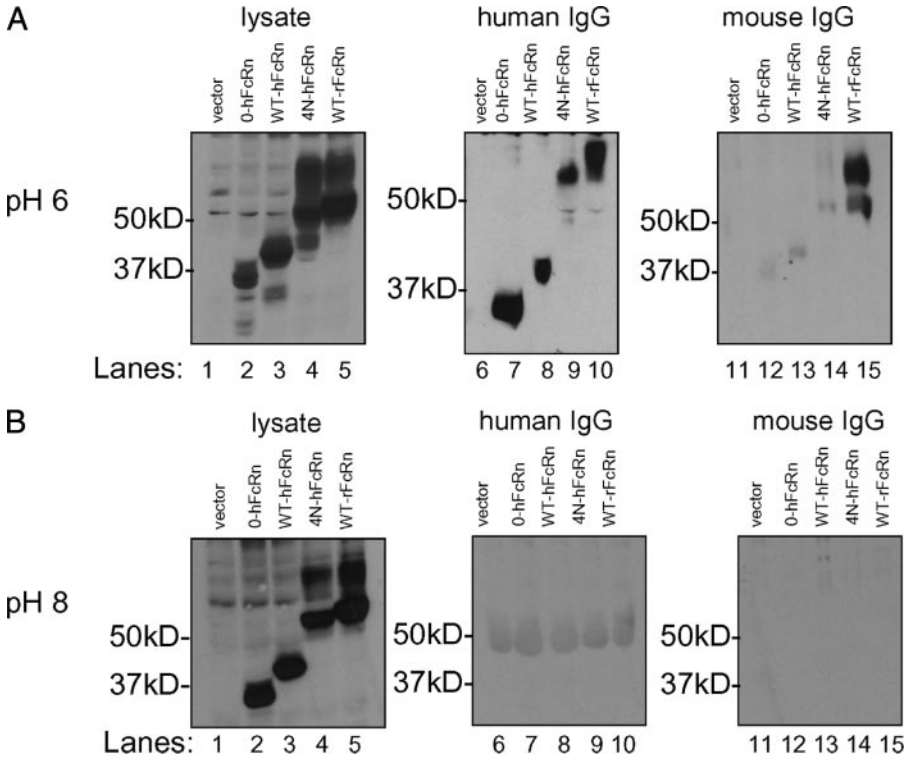

FIGURE 3. **WT-hFcRn and rodentized hFcRn binds to human IgG but not mouse IgG at pH6.** Cells were lysed at CHAPS, pH 6 or pH 8, before incubation with human or mouse IgG and subsequently precipitated with protein G-Sepharose. WT-hFcRn, rodentized hFcRn (4N-hFcRn), and 0-hFcRn were able to bind to human IgG at pH 6 but not pH 8 (*A*, *lanes 7–10*; *B*, *lanes 7–10*). No binding was seen with mouse IgG at either pH (*A*, *lanes 12–14*; *B*, *lanes 12–14*). Only WT-rFcRn bound to mouse IgG at pH6 but not pH 8 (*A*, *lane 15*; *B*, *lane 15*).

Addition of N-Glycan(s) on hFcRn Does Not Confer Binding to Mouse IgG—Previous studies have shown that hFcRn can only bind to IgG from a limited range of species. Specifically, human FcRn can only bind to human and rabbit IgG, whereas rodent FcRn can bind to a broad range of IgG species, including those of mouse, rat, human, and rabbit (11). The fully rodentized hFcRn (4N-hFcRn), along with 0-hFcRn, WT-hFcRn, and WT rFcRn, were used to determine whether addition of *N*-glycan(s) to hFcRn would allow for hFcRn binding to mouse IgG. MDCK II cells expressing these various hFcRn isoforms and rFcRn were lysed in CHAPS at pH 6 or pH 8, and the lysates were subsequently incubated with either human or mouse IgG. Protein G-Sepharose was then added to allow for binding to human or mouse IgG as performed previously (16, 22). Mouse IgG was used rather than rat IgG, because protein G-Sepharose is known to bind poorly to rat IgG. Precipitates of FcRn-IgG-Protein G-Sepharose complexes were resolved by 12% SDS-PAGE under nonreducing conditions. Detection of the HA tag expressed on all hFcRn clones, as defined by immunoblotting with the 12CA5 monoclonal antibody, showed that 0-hFcRn, WT-hFcRn, WT-rFcRn, and the fully rodentized hFcRn (4N-hFcRn) exhibited pH-dependent binding to human IgG at pH 6 (Fig. 3*A*, *lanes 7–10*) but not pH 8 (Fig. 3*B*, *lanes 7–10*). Whereas the mature isoforms of WT-hFcRn, 4N-hFcRn, and WT-rFcRn bound to human IgG at pH 6 (Fig. 3*A*, *lanes 9* and *10*), both the mature and immature isoforms of WT-rFcRn were observed to bind to mouse IgG (Fig. 3*A*, *lane 15*). However, neither the 0-hFcRn, WT-hFcRn, nor fully rodentized hFcRn (4N-hFcRn) demonstrated binding to mouse IgG at either pH 6 (Fig. 3*A*, *lanes 12–14*) or pH 8 (Fig. 3*B*, *lanes 12–14*). Similar observations were made with all the rodentized hFcRn variants and mutant hFcRn clones (1m-, 3m-, and 4m-hFcRn) shown in Fig. 2 in that none were able to bind to mouse IgG (data not shown). rFcRn exhibited pH-dependent binding to both human and mouse IgG at pH 6 (Fig. 3*A*, *lanes 10* and *15*) and not at pH 8 (Fig. 3*B*, *lanes 10* and *15*), as predicted (11). Thus, addition of *N*-glycans to hFcRn to mimic that of rFcRn does not confer cross-species binding to mouse IgG. Interestingly, hFcRn is able to bind to human IgG in the absence of *N*-glycans.

Increased Apical Membrane Surface Expression of Rat FcRn and hFcRn with Addition of N-Glycans—Previous studies have shown that hFcRn localizes predominately to the basolateral surface, whereas rFcRn is distributed to both membrane surfaces (16, 19). To determine the effect of *N*-glycans on the steady-state membrane surface distribution of hFcRn in MDCK II cells, the various transfected clones were grown on Transwells, allowed to polarize before membrane surface labeling with biotin, precipitated with avidin agarose, and subsequently analyzed for protein composition by immunoblotting with the 12CA5 monoclonal antibody. Various amounts of FcRn proteins were detected on both apical and basolateral cell surfaces of MDCK II cells that expressed 0-hFcRn, WT-hFcRn, 4N-hFcRn, and rFcRn (Fig. 4*A*, *lanes 3–10*, *left blots*). Fig. 4*A* (*right blots*) shows immunoblotting of the entire protein lysates analyzed in Fig. 4*A* (*left blots*) with the 12CA5 monoclonal antibody, to detect each of the different FcRn constructs, and β-actin, to demonstrate equal loading (Fig. 4*A*, *lanes 13–20*).

Consistent with our previous studies, the majority of the membrane-bound WT-hFcRn was shown to reside at the basolateral cell surface in comparison to that detected on the apical cell surface (Fig. 4*A*, *lanes 5* and *6*). Similar basolateral membrane distribution was also seen in 0-hFcRn (Fig. 4*A*, *lanes 3* and *4*). The presence of the GP135 marker selectively on the apical surface of all cell lines analyzed (Fig. 4*A*, *left*) showed the fidelity of the biotin labeling, because GP135 is a known apical membrane protein expressed on MDCK II cells. Based upon the quantity of total FcRn detected in the wild-type cell line, it could be estimated that <3% of the total hFcRn was detected at the membrane surfaces as defined by densitometry. Similar results were obtained with the rodentized hFcRn (4N-hFcRn) and WT-rFcRn cell lines in that the majority of FcRn remained intracellular with membrane-bound FcRn ranging from 4% to 10% of the total lysate. The rodentized hFcRn (4N-hFcRn) and the rFcRn transfected contained two species of FcRn (*closed*

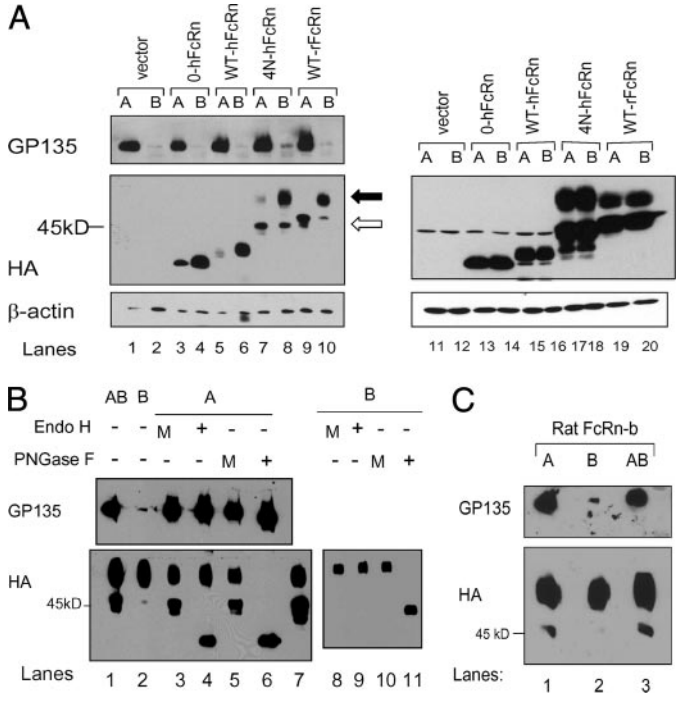

FIGURE 4. **Membrane distribution of FcRn.** Cells were grown on Transwells and allowed to polarize before surface membrane labeling with biotin at the apical (*A*), basolateral (*B*), or both apical and basolateral (*AB*) cell surface(s) and followed by immunoprecipitation with avidin-agarose. Basolateral predominant membrane distributions of FcRn were observed with 0-hFcRn and WT-hFcRn clones (*A*, *lanes 3–6*). Increased apical membrane distribution was observed with 4N-hFcRn and WT-rFcRn (*lanes 7–10*). In both WT-rFcRn and 4N-hFcRn clones, the high mannose isoform of FcRn was distributed to the apical cell surface (*A*, *lanes 7* and *9*, *lower bands*). *Closed arrow* indicates mature isoform, and *open arrow* indicates immature isoform (*A*). Immunoblotting of total lysate with 12CA5 for FcRn is shown (*A*, *lanes 11–20*). Confirmation of membrane bound high mannose and complex *N*-glycan isoforms in 4N-hFcRn were performed using Endo H, PNGase F, or mock (*M*) digestion (*B*). A separate rat FcRn clone (*rat FcRn-b*) had also been generated (*C*). Membrane protein isolation from apical (*A*), basolateral (*B*), and both apical and basolateral (*AB*) surfaces demonstrated the presence of rat FcRn at both membrane surfaces. Different from the clone in *A* (*lanes 9* and *10*), this clone showed that the mature isoform was visible in both membrane surfaces (*C*, *lanes 1* and *2*).

and *open arrows* in Fig. 4*A*, *lanes 7–10*) at the membrane surfaces. Given the findings in Fig. 2*C*, it was hypothesized that the upper band (*closed arrowhead*) represented a mature species of FcRn with complex *N*-glycans and the lower band (*open arrow*) represented an immature species of FcRn with high mannose glycan isoforms. It was also notable that the rodentized hFcRn and rat FcRn displayed enhanced expression on the apical cell surface relative to that observed on the apical cell surface of the non-glycosylated (0-hFcRn) and WT-hFcRn isoforms (compare Fig. 4*A*, *lanes 3*, *5*, *7*, and *9*). Moreover, whereas the basolateral cell surface of the MDCK II cells contained predominantly the high molecular weight (mature, complex *N*-glycan) species, both lower molecular weight (immature, high mannose *N*-glycan) and higher molecular weight (mature *N*-glycan) species of FcRn were observed on the apical cell surface of both the rodentized hFcRn (4N-hFcRn)- and rat FcRn-transfected cell lines (WT-rFcRn) (Fig. 4, *A* (*lanes 7* and *8*), *B* (*lanes 3–5*), and *C* (*lane 1*)). These studies suggest that increased glycosylation of hFcRn altered its polarity of expression to more resemble that observed with rat FcRn with an increase in apical membrane expression as compared with that observed with WT-hFcRn, which exhibited a strong basolateral predominance of hFcRn expression.

A separate rodentized hFcRn (4N-hFcRn) transfectant also showed increased apical membrane expression of mature and immature FcRn (Fig. 4*B*, *lane 3*) relative to the basolateral surface, which primarily expressed mature FcRn (Fig. 4*B*, *lane 2*). To confirm that the upper and lower bands represented mature and immature isoforms of the rodentized hFcRn (4N-FcRn), respectively, biotin-labeled membrane 4N-hFcRn clones were immunoprecipitated with avidin-agarose and subsequently subjected to digestion with Endo H or PNGase F before resolving on 12% SDS-PAGE followed by immunoblotting for FcRn and GP135. Significantly more protein was used in this experiment, and, as with previous experiments, equivalent amounts of protein were added to each lane. These studies demonstrated the presence of both immature and mature FcRn isoforms at the apical membrane (Fig. 4*B*, *lane 3*). In the presence of Endo H, the lower band migrated to 37 kDa, which is consistent with the location of the deglycosylated FcRn (Fig. 4*B*, *lane 4*). In the presence of PNGase F, only the deglycosylated hFcRn was detectable (Fig. 4*B*, *lane 6*). Protein isolated from biotin-labeled basolateral membrane showed the presence of only mature 4N-hFcRn (Fig. 4*b*, *lane 8*). Confirmation of the complex *N*-glycan (mature) isoform was shown by resistance to Endo H digestion (Fig. 4*B*, *lane 9*) and by sensitivity to PNGase F digestion (Fig. 4*B*, *lane 11*).

To determine whether this apical redistribution of the rodentized hFcRn (4N-hFcRn) was also observed with other hFcRn isoforms created (see supplemental Fig. S2), we performed the following series of studies on MDCK II cells expressing hFcRn containing one and two additional *N*-glycan carbohydrate modifications within the α1, α2, and/or α3 domains. MDCK II cells that expressed these various combinations and numbers of *N*-glycans were biotin-labeled on the apical, basolateral, or both cell surfaces. Protein lysates from these cells were precipitated with avidin-agarose, and the precipitates were analyzed for the presence of FcRn or an apical marker (GP135) by immunoblotting with the 12CA5 or GP135 antibodies, respectively (supplemental Fig. S3). The upper blots confirmed the fidelity of the biotin labeling given the exclusive detection of GP135 on the apical cell surface. As previously observed with the fully rodentized hFcRn (4N-hFcRn), all hFcRn clones with additional *N*-glycan(s) exhibited enhanced expression of FcRn at the apical cell surfaces (supplemental Fig. S3, *lanes 4*, *7*, *10*, *13*, *16*, and *19*). In addition, both immature and mature isoforms were detected at the apical surfaces of all FcRn clones with one additional *N*-glycan carbohydrate modification (1-FcRn, 3-hFcRn, and 4-hFcRn) (supplemental Fig. S3, *lanes 4*, *7*, and *10*). Similar to the fully rodentized (4N) hFcRn clone, hFcRn clones with three *N*-glycans (123-, 124-, and 234-hFcRn) exhibited increased FcRn expression at the apical cell surface (supplemental Fig. S3, *lanes 13*, *16*, and *19*) relative to the basolateral cell surface (supplemental Fig. S3, *lanes 14*, *17*, and *20*). These studies show that no specific *N*-glycan location or combination determined apical redistribution but rather appeared to be related to the total amount of *N*-glycan contained within FcRn.

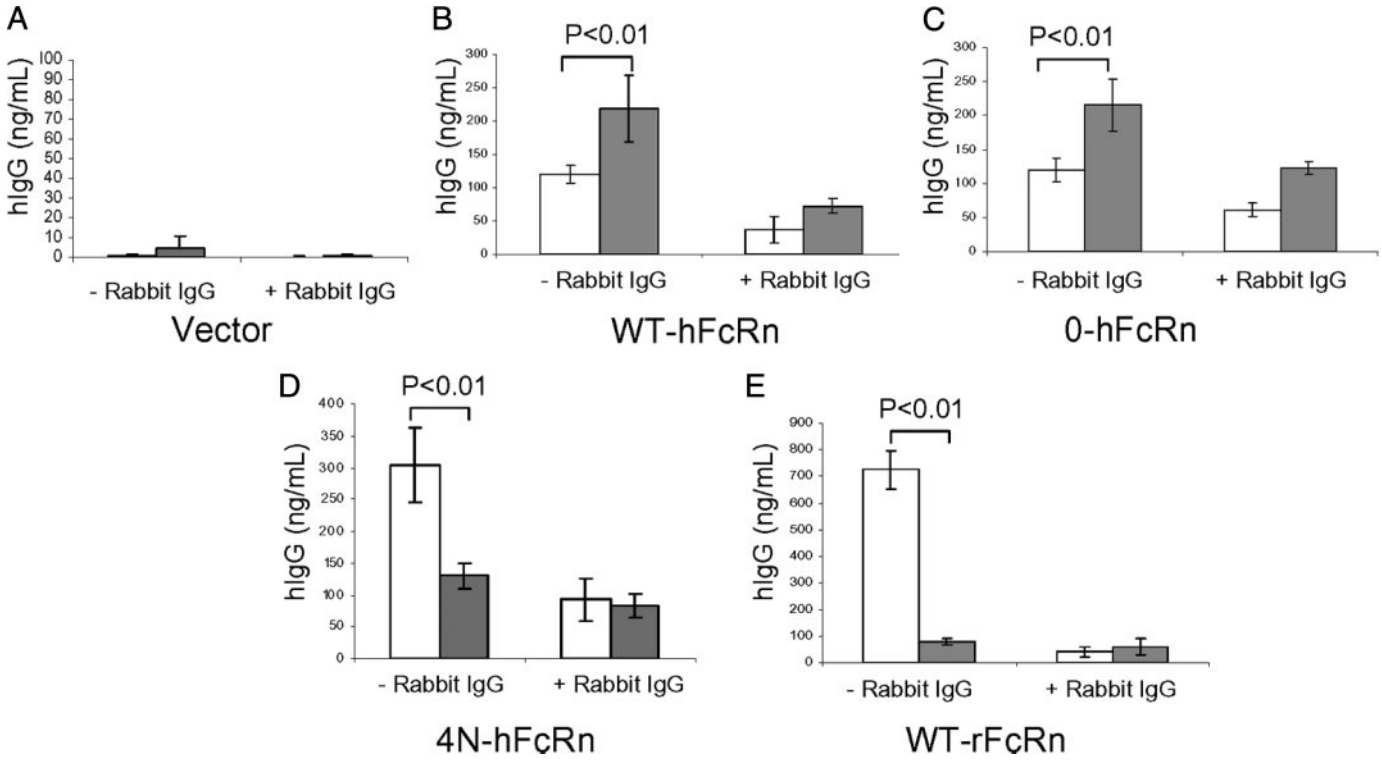

FIGURE 5. **Reversal of human IgG transport with full rodentization of hFcRn.** Bidirectional hIgG transport, apical to basolateral (*white bars*) and basolateral to apical (*gray bars*), was observed in all clones, except for Vector clone (negative control), which does not express FcRn (*A*). 0-hFcRn clone exhibited similar basolateral-to-apical direction of hIgG transport (*C*) as that of WT-hFcRn (*B*). 4N-hFcRn clone displayed predominate apical-to-basolateral hIgG transport (*D*), similar to that of WT-rFcRn (*E*). Addition of rabbit IgG significantly decreased hIgG transport in all clones.

Reversal of Vectoral Direction of IgG Transport in Rodentized Human FcRn—It has been previously demonstrated that wild-type hFcRn when expressed in MDCK II cells preferentially directs hIgG transport from the basolateral to the apical surface and less so from the apical to the basolateral cell surface (16, 17, 22). It has also been previously noted that rat FcRn exhibits a reversal of this polarity of transcytosis with the major vector of IgG movement being apical-to-basal (20, 24, 25). We therefore examined whether rodentization of hFcRn, which was associated with apical redistribution of hFcRn similar to that of rat FcRn, was also associated with a vector of IgG transport that would resemble rat FcRn.

To examine the preferential direction of IgG transport, transfected MDCK-II cells were therefore cultured on Transwell membranes and allowed to polarize. Because human (h) IgG was shown to bind various rodentized hFcRn and rat FcRn, we assessed hIgG transport function of a selected hFcRn clones as well as rFcRn (11). hIgG was added to the input chamber, which was buffered to pH 6 to enhance hIgG binding, with or without rabbit IgG, which can bind competitively to both human and rat FcRn as a means to compete with hIgG transport as previously performed (16, 22). The output chamber medium, which was buffered to pH 7.4 to enhance FcRn dissociation from IgG, was sampled after 120 min, and the hIgG concentrations were determined in the output chamber by enzyme-linked immunosorbent assay. Bidirectional hIgG transport was detected in MDCK II cells transfected with wild-type hFcRn (WT-hFcRn), fully rodentized hFcRn (4N-hFcRn), non-glycosylated hFcRn (0-hFcRn), and rat FcRn (WT-rFcRn). Consistent with previous studies, WT-hFcRn was observed to direct hIgG predominantly from the basolateral-to-apical direction (Fig. 5*B*) (16). Specificity for transport was shown by the ability of rabbit IgG, which can bind to hFcRn, to significantly block this bidirectional transport (Fig. 5*B*). Removal of the single *N*-glycan from hFcRn did not alter the predominant direction of hIgG transport or its blockade by rabbit IgG (Fig. 5*C*). However, when hFcRn was fully rodentized (Fig. 5*D*), its predominant direction of transport of hIgG was reversed and identical to that of rat FcRn (Fig. 5*E*), which was predominately in the apical-to-basal direction. Therefore, rodentization of hFcRn altered the vectoral direction of hIgG transport in a manner that made hFcRn function similarly to the rodent isoform.

DISCUSSION

Little is known about the regulation of FcRn trafficking in epithelial cells with most of the knowledge deriving from an assessment of the role of the cytoplasmic tail in rodents and human. Drawing from the differences in the specific details of the functional and structural differences between rodents and humans, we sought to focus on the dissimilarities between the carbohydrate side-chain modifications expressed on rodent and human FcRn, and how these might relate to the global differences in FcRn distribution and function observed between these two isoforms; namely the important differences observed in cross-species IgG binding, membrane polarity of FcRn expression, and the vectoral direction of IgG transport. We hypothesized that these functional differences may allow for an interrogation of the manner in which FcRn structure

regulates function. We therefore generated a wide variety of human isoforms that were mutated to possess asparagine residues positioned to impose *N*-glycan carbohydrate side-chain modifications in hFcRn with the characteristic of the rodent isoform.

Consistent with previous studies, we observed that, when expressed in MDCK II cells with hβ2m, wild-type hFcRn consisted of both high mannose and complex carbohydrate containing isoforms as defined by sensitivity to Endo H and PNGase F. However, also consistent with previous studies, the majority of wild-type hFcRn that was displayed on the cell surface consisted predominantly of a mature glycoprotein that was predominantly sorted to the basolateral surface (16, 22). Various isoforms of rodentized hFcRn through addition of multiple combinations of *N*-linked carbohydrate side-chain modifications were also characterized by the expression of both high mannose and complex *N*-glycan carbohydrate isoforms, as was wild-type rat FcRn, when expressed in MDCK II cells. In contrast to WT-hFcRn, the various rodentized hFcRn isoforms exhibited increased apical expression of both immature and mature hFcRn isoforms. Of these, the expression of mature hFcRn isoforms at the apical cell surface is functionally relevant given the binding of mature isoforms to human IgG and basally directed transcytosis from the apical surface as shown here. The expression of immature glycoproteins at the apical cell surface is interesting but must be currently viewed as being functionally irrelevant given the lack of binding to human IgG and the absence of immature rat FcRn glycoproteins in non-transfected cell lines expressing endogenous levels of FcRn (supplemental Fig. S4, *lanes 5–7*). Thus, the addition of *N*-linked carbohydrate side-chain modifications to hFcRn confers increased mobilization to the apical cell surface and the reversal of IgG transcytosis typical of rFcRn.

N-Glycans have been proposed to play a role in FcRn binding to IgG. The crystal structure of rFcRn in combination with rat (r) IgG has shown that *N*-glycans in rFcRn are at the interaction sites with IgG, and it has been hypothesized that the FcRn dimer is stabilized through a "carbohydrate handshake" (14). The *N*-glycan carbohydrate at Asn-128 of rFcRn specifically contacts rat Fc (13). Based upon these findings, studies using surface plasmon resonance have shown that mutation of Leu-137 in hFcRn to Glu-137 (as seen in mouse FcRn) and rodentization of residues 79–89 (areas that also encompass the proposed mouse *N*-glycosylation site at the α1 domain) resulted in increased mIgG1, mIgG2a, and mIgG2b binding (12). However, this interaction was not as strong as mFcRn binding to mIgG, and the affinity to hIgG1 was in turn reduced 2-fold. Further studies have shown that mutation of hFcRn at amino acid residues 136–147 (an area that is outside of the *N*-glycan site) to mimic that of mouse FcRn resulted in increase binding to mIgG1 and mIgG2b, and this binding was enhanced with additional mutations of hFcRn at amino acid residues 79–89 to mimic that of mFcRn (26). The sites of these mutations have suggested that the *N*-glycan carbohydrate of mFcRn at residues 87 and 128 of rFcRn (*N*-glycans positions 1 and 3 on supplemental Figs. S1 and S2) may play a role in IgG binding. However, the rodent IgG binding studies with the mutated hFcRn isoforms studied here did not reveal increased binding of mouse IgG. The differences in our studies in comparison to the previously published studies may be the following. In the current study, polyclonal mouse IgG was used as opposed to specific IgG isotypes performed previously. Another possibility is that because we only added asparagine residues, the *N*-glycan carbohydrate modifications alone may not contribute to cross-species binding alone but may depend on the contribution of neighboring residues that were not modified in the current study. It is also possible that stronger binding is required to detect differences in binding using protein G-Sepharose precipitation assays as opposed to surface plasmon resonance. Overall, addition of *N*-glycans to hFcRn did not reveal significant changes in binding of hFcRn to mouse IgG.

Although *N*-glycans have been shown by some studies to function as an apical targeting signal in polarized epithelia, it may not be the dominant factor in the regulation of apical membrane trafficking (27). For example, removal of *N*-glycans in hepatitis virus B antigen or soluble ectodomain of p75 neurotrophin receptor does not alter the apical sorting pattern (28, 29). In our study, addition of even one *N*-glycan at any position of hFcRn (1-, 3-, and 4-hFcRn) enhanced the redistribution of FcRn to the apical surface compared with that of WT-hFcRn, which localizes predominantly to the basolateral surface. With one or two additional *N*-glycans at any position (123-, 124-, and 234-hFcRn), there was a marked membrane targeting to the apical surface, similar to that of the fully rodentized hFcRn (4N-hFcRn) and WT-rFcRn. This redistribution of hFcRn was similar to the steady-state levels of wild-type rat FcRn as observed in transfected MDCK II and inner medullary collecting duct cells in two previous studies (20, 24). Interestingly, an analysis of the fully rodentized hFcRn (4N-FcRn) in comparison to wild-type hFcRn also showed an increase in the relative amount of membrane bound to intracellular FcRn. These data suggest that the *N*-glycans may play a significant role in mediating apical membrane distribution of FcRn and enhancing either stabilization of FcRn on the cell surface and/or movement of FcRn to the cell surface. However, the apical membrane distribution is not determined by a specific *N*-glycan, and the ratio of apical-to-basolateral membrane distribution is not simply a cumulative effect of the numbers of *N*-glycans.

The increased redistribution of rodentized hFcRn to the apical cell surface in a distribution that was similar to that of wild-type rFcRn raised the possibility that this may be reflected physiologically in an alteration of the vectoral direction of IgG transport that was also similar to rat FcRn: specifically, a predominantly apical-to-basal direction of transport. Previous studies of rFcRn when expressed in the inner medullary collecting duct cell line showed bidirectional transcytosis of rat IgG, but the predominant direction of IgG transport was not determined (18). Tesar and colleagues, however, showed that rFcRn, when expressed in MDCK II cells, transported more rat Fc and rat IgG in the apical-to-basal direction (20). Similarly, in our study using MDCK II cells that expressed both rFcRn and rβ2m, we observed bidirectional transcytosis of human IgG, which is known to bind to rodent FcRn with a predominant apical-to-basolateral direction of IgG transport.

Consistent with our previous study, wild-type hFcRn in MDCK II cells also exhibited bidirectional human IgG trans-

port with predominantly basal-to-apical direction (16). In marked contrast, the fully rodentized hFcRn mutant isoform exhibited a reversal of this polarity that matched the vector of polarity of protein expression on the cell surface membranes, and it exhibited bidirectional transport with a predominantly apical-to-basal direction of transport, which was the same as that of rFcRn. The similarity between the wild-type rFcRn and fully rodentized hFcRn strongly supports a role of *N*-glycans in determining the sorting of FcRn expression and direction of IgG transport.

In wild-type hFcRn, the cytoplasmic tail has been believed to be critical in determining the predominant basolateral membrane distribution and basolateral-to-apical hIgG transport (16). The cytoplasmic tail of rat FcRn likely has a similar basolateral targeting function, because mutant rFcRn without a cytoplasmic tail also results in a redistribution to the apical cell surface (19). Thus, the *N*-glycan carbohydrates on the wild-type rFcRn and the fully rodentized hFcRn appear to counter the trafficking imposed by the cytoplasmic tail, which directs sorting of FcRn to the basolateral cell surface. An interesting possibility is that IgG binding to FcRn may mask the *N*-glycan apical signals allowing the cytoplasmic basolateral motifs to be temporarily dominant. Upon exposure to the pH-neutral basolateral surface, the release of bound IgG re-exposes the *N*-glycans allowing them to function yet again as apical sorting signals. Whether this role of the *N*-glycan carbohydrate regulates apical membrane trafficking through intracellular lectin receptor interactions (such as VIP-36), or whether *N*-glycans negatively regulate a basolateral sorting pathway remains to be defined (27). Interestingly, in this regard, is the fact that our studies suggest that *N*-glycans strongly contributed to apical membrane distribution and the predominant vector of IgG transport. Our observations with rodentized human FcRn also allow us to make other predictions about the physiological function of *N*-glycans in normal rat FcRn biology. It is important to point out that the increased numbers of *N*-glycans on rodent FcRn may have additional benefits to the physiologic function of FcRn in rodents. The allowance for increased apical-to-basal transport imposed by increased *N*-glycans will facilitate the passive acquisition of IgG by neonatal rodents that is a hallmark function of this receptor (1). In addition, it can be envisioned that addition of *N*-glycans to rodent FcRn might allow improved function in the hostile environment of the apical cell surface.

These studies thus demonstrate that addition of *N*-glycans to hFcRn does not confer cross-species binding to rodent IgG but, rather, results in a redistribution of hFcRn to the apical membranes and reversal of hIgG transport across MDCK II cells that make the fully rodentized hFcRn resemble wild-type rFcRn. These data suggest that the *N*-glycans in rat FcRn play a significant role in the steady-state membrane surface distribution and the direction of IgG transport that is mediated by FcRn.

Acknowledgment—We thank Daniel Bailey for technical assistance.

REFERENCES

1. Brambell, F. W. (1969) *Proc. Nutr. Soc.* **28,** 35–41
2. Simister, N. E., and Mostov, K. E. (1989) *Cold Spring Harbor Symp. Quant. Biol.* **54,** 571–580
3. Yoshida, M., Masuda, A., Kuo, T. T., Kobayashi, K., Claypool, S. M., Takagawa, T., Kutsumi, H., Azuma, T., Lencer, W. I., and Blumberg, R. S. (2006) *Springer Semin. Immunopathol.* **28,** 397–403
4. Burmeister, W. P., Huber, A. H., and Bjorkman, P. J. (1994) *Nature* **372,** 379–383
5. Rodewald, R., Lewis, D. M., and Kraehenbuhl, J. P. (1983) *CIBA Found. Symp.* **95,** 287–299
6. Gill, R. K., Mahmood, S., Sodhi, C. P., Nagpaul, J. P., and Mahmood, A. (1999) *Indian J. Biochem. Biophys.* **36,** 252–257
7. Roopenian, D. C., and Akilesh, S. (2007) *Nat. Rev. Immunol.* **7,** 715–725
8. Mi, W., Wanjie, S., Lo, S. T., Gan, Z., Pickl-Herk, B., Ober, R. J., and Ward, E. S. (2008) *J. Immunol.* **181,** 7550–7561
9. Yoshida, M., Claypool, S. M., Wagner, J. S., Mizoguchi, E., Mizoguchi, A., Roopenian, D. C., Lencer, W. I., and Blumberg, R. S. (2004) *Immunity* **20,** 769–783
10. Qiao, S. W., Kobayashi, K., Johansen, F. E., Sollid, L. M., Andersen, J. T., Milford, E., Roopenian, D. C., Lencer, W. I., and Blumberg, R. S. (2008) *Proc. Natl. Acad. Sci. U. S. A.* **105,** 9337–9342
11. Ober, R. J., Radu, C. G., Ghetie, V., and Ward, E. S. (2001) *Int. Immunol.* **13,** 1551–1559
12. Zhou, J., Johnson, J. E., Ghetie, V., Ober, R. J., and Ward, E. S. (2003) *J. Mol. Biol.* **332,** 901–913
13. Martin, W. L., West, A. P., Jr., Gan, L., and Bjorkman, P. J. (2001) *Mol. Cell* **7,** 867–877
14. Vaughn, D. E., and Bjorkman, P. J. (1998) *Structure* **6,** 63–73
15. Scheiffele, P., Peranen, J., and Simons, K. (1995) *Nature* **378,** 96–98
16. Claypool, S. M., Dickinson, B. L., Wagner, J. S., Johansen, F. E., Venu, N., Borawski, J. A., Lencer, W. I., and Blumberg, R. S. (2004) *Mol. Biol. Cell* **15,** 1746–1759
17. Dickinson, B. L., Claypool, S. M., D'Angelo, J. A., Aiken, M. L., Venu, N., Yen, E. H., Wagner, J. S., Borawski, J. A., Pierce, A. T., Hershberg, R., Blumberg, R. S., and Lencer, W. I. (2008) *Mol. Biol. Cell* **19,** 414–423
18. McCarthy, K. M., Lam, M., Subramanian, L., Shakya, R., Wu, Z., Newton, E. E., and Simister, N. E. (2001) *J. Cell Sci.* **114,** 1591–1598
19. Wu, Z., and Simister, N. E. (2001) *J. Biol. Chem.* **276,** 5240–5247
20. Tesar, D. B., Tiangco, N. E., and Bjorkman, P. J. (2006) *Traffic* **7,** 1127–1142
21. Stefaner, I., Praetor, A., and Hunziker, W. (1999) *J. Biol. Chem.* **274,** 8998–9005
22. Claypool, S. M., Dickinson, B. L., Yoshida, M., Lencer, W. I., and Blumberg, R. S. (2002) *J. Biol. Chem.* **277,** 28038–28050
23. Ho, S. N., Hunt, H. D., Horton, R. M., Pullen, J. K., and Pease, L. R. (1989) *Gene* (*Amst.*) **77,** 51–59
24. McCarthy, K. M., Yoong, Y., and Simister, N. E. (2000) *J. Cell Sci.* **113,** 1277–1285
25. Kim, K. J., Fandy, T. E., Lee, V. H., Ann, D. K., Borok, Z., and Crandall, E. D. (2004) *Am. J. Physiol.* **287,** L616–L622
26. Zhou, J., Mateos, F., Ober, R. J., and Ward, E. S. (2005) *J. Mol. Biol.* **345,** 1071–1081
27. Rodriguez-Boulan, E., and Gonzalez, A. (1999) *Trends Cell Biol.* **9,** 291–294
28. Yeaman, C., Le Gall, A. H., Baldwin, A. N., Monlauzeur, L., Le Bivic, A., and Rodriguez-Boulan, E. (1997) *J. Cell Biol.* **139,** 929–940
29. Marzolo, M. P., Bull, P., and Gonzalez, A. (1997) *Proc. Natl. Acad. Sci. U. S. A.* **94,** 1834–1839